EFFECTS OF TRACE METALS ON PARTICULATE MATTER FORMATION IN A DIESEL ENGINE: METAL CONTENTS FROM FERROCENE AND LUBE OIL

D. G. LEE[1)*], A. MILLER[2)], K. H. PARK[3)], and M. R. ZACHARIAH[4)]

[1)]School of Mechanical Engineering, RIMT, Pusan National University, Busan 609-735, Korea
[2)]NIOSH/Spokane Research Lab, WA 99207, USA
[3)]Department of Environmental Science and Engineering, Gwangju Institute of Science and Technology, Gwangju 500-712, Korea
[4)]Department of Mechanical Engineering and Department of Chemistry and Biochemistry, University of Maryland, MD 20742, USA

ABSTRACT−Diesel particulate matter (DPM) often contains small amounts of metal as a minor component but this metal may contribute to adverse health effects. Knowledge of the mechanism for particle formation as well as the size preference of the trace metals is critical to understanding the potential for health concerns. To achieve this, the size and the composition of each particle should be optimally measured at the same time. Single particle mass spectrometer (SPMS) would be the best tool for this objective. In this paper, we therefore will introduce new findings about the mechanism and distribution of the trace metals in DPM, derived from a study where an SPMS was used to analyze freshly emitted DPM.

KEY WORDS : Single particle mass spectroscopy, Diesel particulate matter, Characterization, Metal contents

1. INTRODUCTION

Diesel Engines emit a tri-modal size distribution of Diesel particulate matter (DPM) at concentrations as high as 10^9 particles/cm^3 (Kittelson, 1998). Ultrafine particles i.e. the nuclei- and accumulation-mode particles are known to be the most harmful because of their deep penetration and easy deposition into the human lung. Also coarse-mode DPM often contains alkali and transition metal species such as Ca, Al, Na, Ba, Zn, Fe, Se, Mg and so on (Gross *et al.*, 2000). It has been thought that the Diesel-generated metals originate from lube oil via the reverse blow-by process, mechanical wear of break pads, and combustion of metal-containing fuel additives such as ferrocene or cerium. But, there have been no reports to give answers to the following questions: how much metal is in a particle (single particle analysis of metals), whether or not metal contents are uniformly distributed in size (size preference of metals), and how and where they form (mehanism of metal formation). These fundamental questions motivate this research.

Recent interest in adverse health effects of DPM initiated research relevant to in-situ measurement of the size of DPM at various engine modes. For example, Kittelson and Zachariah's group have reported that metal content in DPM plays a catalytic role in carbon oxidation inside the engine or even in a flame, using tandem differential mobility analyzer (TDMA) (Kim *et al.*, 2005a; Jung *et al.*, 2005; Higgins *et al.*, 2003, Kim *et al.*, 2005b).

Hence, the technology for sizing nanoparticles seems to be well established, while in-situ quantitative single *nanoparticle* mass and size analysis doesn't do that to date. An ideal tool if it exists should be capable of simultaneously measuring the size and chemical composition of single nanoparticles. Aerosol time-of-flight mass spectroscopy (AMS) might be the closest approximation to such a tool. The Prather group indeed reported the simultaneous measurement of size and composition of particles (Noble and Prather, 2000).

But, as AMS employs light scattering for sizing particles as well as triggering the ionizing laser, the measurable size of particles are often limited to those larger than 200nm. This hinders the use of that machine to analyze the nuclei- and accumulation-mode particles that are

more important in terms of the potential for adverse health effects. Also the power of the conventional laser installed in the AMS may appear to be not enough for complete ionization of a particle, because the resulting mass spectra consist of only molecular positive and negative ions. The different polarity of such ions facilitates the rapid recombination and charge transfer between ions with larger ionization potential (IP) and those with less IP (Mahadevan *et al.*, 2002). This yields some bias in the measured composition of the particle. For this reason, the majority of research has focused on reporting the qualitative rather than quantification assignment of molecular species composing an environmental particle.

We recently showed that the use of a much stronger laser pulse seemed very likely to solve these problems (Lee *et al.*, 2005). Also we demonstrated that the SPMS with the capability of simultaneous measurement of size and composition of particles could be used to elucidate various nanoscale phenomena, for example, finding solid state reaction kinetics inside a nanoparticle (Mahadevan *et al.*, 2002), and size-resolved surface reaction kinetics (Park *et al.*, 2005). In this study, we applied the SPMS to explore the composition of DPM, namely the origin of metals and size preferences of metals originating from metallic fuel additives and lube oil. In addition, we extract statistical data from the single particle analyses and eventually, address the mechanism of formation of metals.

2. EXPERIMENTAL PROCEDURE

Our SPMS consists of an aerodynamic inlet, a source region for particle-to-ion conversion with a free firing high powered Nd:YAG laser, a linear time-of-flight (TOF) tube and a multichannel plate detector (MCP), as shown in Figure 1. The aerodynamic lens inlet is employed to separate particles from the carrier gas and collimate them such that they can be injected through differentially pumped chambers to the ionization region, albeit with some traveling losses en route. As configured, positive ions formed from a particle by multi-photon laser ionization are accelerated along the ~1 m long linear TOF tube and detected with the MCP. More details regarding this SPMS design are described elsewhere (Mahadevan *et al.*, 2002; Lee *et al.*, 2005; Park *et al.*, 2005).

The source of diesel particulate for this work was an Onan-Cummins "QuietDiesel" genset powered by a three cylinder, 1.5 liter Isuzu engine. This unit is capable of providing 10 kW of continuous AC power at a fuel flow rate of about 4 kg/hr. In order to maintain a steady 60 Hz of AC current from the generator, the fuel flow to the engine is controlled by an electronic governor actuator that maintains a constant engine speed of 1800 rpm. The load on the engine is provided by loading the generator

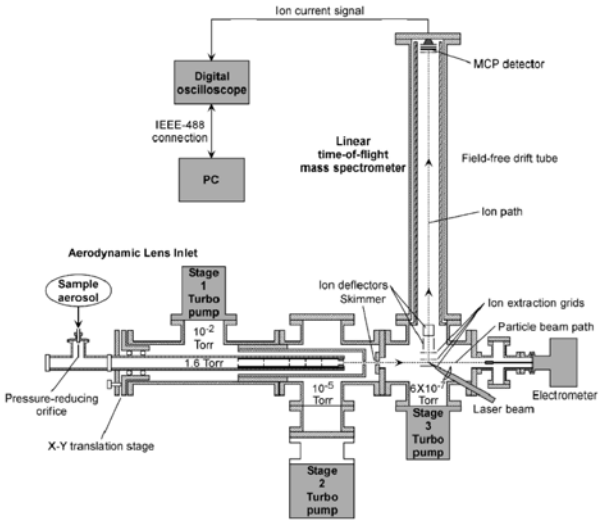

Figure 1. Schematic of single particle mass spectrometer.

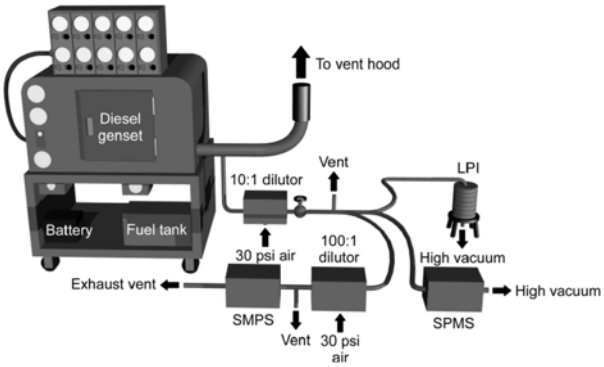

Figure 2. Sampling and dilution of DPM using exhaust probe and ejector dilutor.

outlet with a resistive load bank made by the Simplex Company.

For most of our experiments, the engine was run at two conditions i.e. no-load and 6 kW load unless otherwise noted. The corresponding fuel flow rates were 1.0 kg/hr and 2.25 kg/hr. It should be noted that the size distribution of particles generated by this relatively small engine varies somewhat from that of typical heavy-duty engines. Under normal operating conditions it produces no discernable nuclei mode and the accumulation mode decreases with engine load rather than increases as it does for most larger engines (Kittelson, 1998).

Sampling of exhaust gases and DPM was accomplished using a probe of 3 mm ID inserted into the 10 cm ID exhaust tube. The samples were diluted using an ejector-type dilutor. Cold-flow calibration using a bubble flow meter at the dilutor inlet and a rotameter at the outlet, yielded a dilution ratio of approximately 10:1 for this setup. For measurements of particle size distribution with

the SMPS, the flow was further diluted as shown in Figure 2, using a second ejector dilutor. To investigate the effects of metals on DPM formation, we first added ferrocene to the fuel as an iron source, the amount of which was varied from 20 ppm to 60 ppm. Secondly 1% lube oil (SAE 15W-40) was directly doped to the fuel tank to see the effect of enhancing the level of metallic lube oil additives that might result through the reverse blow-by process. The amount of doped metals is too large to simulate normal lube oil consumption, but is used as a means of adding metals to particles to elucidate the catalytic effect.

3. EFFECTS OF METALS ON DPM SIZE

As described in the previous section, we tested two metal sources such as ferrocene and lube oil. First we would like to show the effect of the ferrocene on DPM size. Figure 3a shows that when the fuel is doped with 60 ppm iron, the size distribution of particles contains a distinct nuclei mode that increases with engine load. This increase in self-nucleated metal particles reflects higher metal throughput, since the increase in load results in higher fuel flow rates and thus higher metal throughput. As the doping rate is reduced to 20 ppm (Figure 3(b)), the iron content is lowered and the nuclei mode eventually disappears at 0 kW engine load as illustrated in the figure.

For both doping levels (Figures 3(a) and 3(b)), the size distribution is strongly bimodal in the range measured by

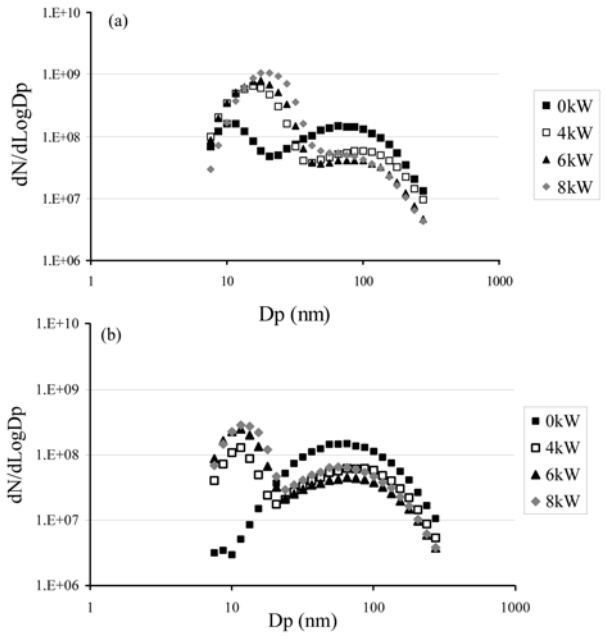

Figure 3. Size distributions of DPM at various engine loads which is doped with (a) 60 ppm Fe and (b) 20 ppm Fe.

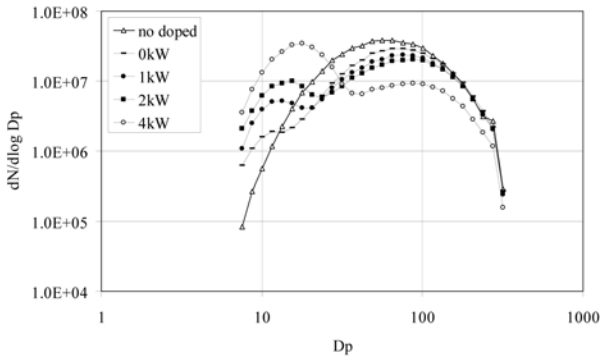

Figure 4. Size distributions of DPM at various engine loads which is doped with 1% lube oil.

the SMPS and the diluted-corrected total number concentrations vary from about 5×10^7 #/cc to about 5×10^8 #/cc (higher numbers being reflective of the increasing number of nuclei mode particles at high engine load). The accumulation mode particles are shown to decrease as load (and thus both engine temperature and metal content) goes up, especially during the initial increase from 0 kW to 4 kW load.

When 1% lube oil is doped to the fuel, the nuclei mode of DPM begins to appear even at the relatively low engine load of 1 kW (see Figure 4). More clearly, the figure verifies the gradual decrease in the number of the accumulation mode particles with the engine load. The overall trend of changes in the size distribution is very similar to that in Figure 3. Despite this, we note that there is a remarkable difference between the cases of ferrocene and lube oil. For 1% doping of lube oil, more than 1000 ppm of the total metals are doped to the diesel fuel, which is much higher than in the ferrocene case (see table 1). Much higher levels of metals may enhance carbon oxidation in the engine, leading to reduction in number of preexisting carbon particles (Jung *et al.*, 2003). In turn, gaseous metals do not find sufficient sites for condensation. It is probable that the metals instead tend to self-nucleate. The self-nucleation process should be pronounced at higher doses of metals, i.e. in the lube oil case, which may explain the more pronounced nuclei mode. In this case, increased number of nuclei particles may lead to vigorous coagulation between themselves and with accumulation mode particles. The same trend was observed by Kyto *et al.* (2002).

4. COMPOSITIONAL ANALYSIS OF DPM

4.1. Classes of DPM according to Mass Spectra

The nuclei mode of DPM is generally considered to consist of two particle types; nonvolatile inorganic ash that nucleates at high temperatures in the engine (Kittelson *et al.*, 2002), and condensed volatile materials

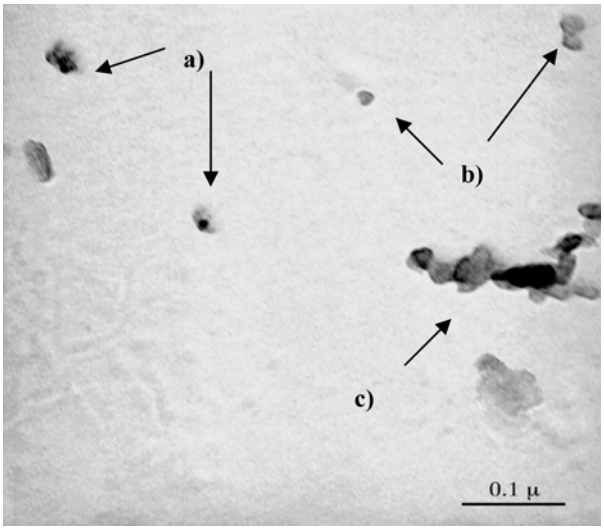

Figure 5. TEM images representing the three classes of DPM doped with Fe at 6 kW load and 60 ppm doping.

such as sulfates and unburned fuel or oil vapors which self nucleate later during the dilution/cooling of the exhaust aerosol (Sakurai *et al.*, 2003). The accumulation mode on the other hand, which would be the third type of particle, is said to consist mainly of "spherules" i.e. primary particles of elemental carbon, coagulated into agglomerates, with other materials adsorbed onto the surface. Particle mass spectra are sorted into two classes according to the ratio of hydrogen (H) to carbon (C) as a criterion, i.e. organic carbon (OC when H/C > 1) and elemental carbon (EC when H/C < 1). The third class is pure metal where metal to carbon ratio is larger than 10. These are metal nanoparticles (presumably self-nucleated in the engine). Figure 5 shows distinct differences in morphology and size for the three classes of particles generated during combustion of iron-doped fuel.

The dark spot of the figure, say (a), corresponds to Fe rich particles, i.e. the third class, which was confirmed by energy dispersive X-ray spectroscopy (EDS). The non-agglomerate light gray particles of (b) are organic carbon, while large agglomerates of (c) contain elemental carbon and iron as well, which is attributed to coagulation between them. Typical mass spectra also show consistently the variation in composition of the three classes (not shown here).

The classification process was also carried out for the case of combustion of lube-oil doped fuel. According to Table 1, the oil contains various metals, so one may predict that TEM images and EDS of the DPM should show a composite of the four metal elements such as S, Ca, Zn, and P. Also the relative abundance of each element in such composites may be expected to decrease in that order. But, surprisingly, the particle mass spectra

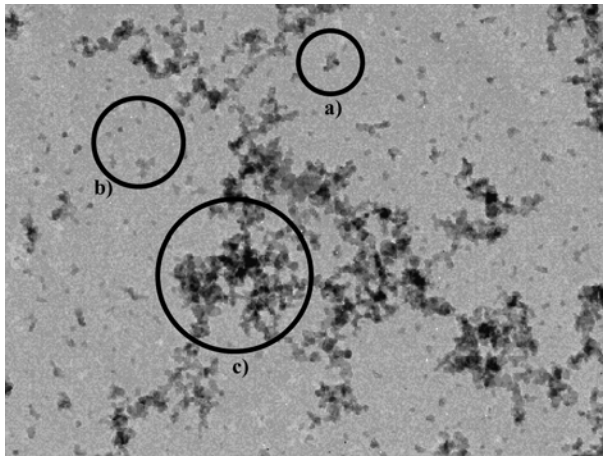

Figure 6. TEM images representing the three classes of DPM doped with 1% lube oil at 6 kW engine load.

Table 1. Elemental components and their properties of lube oil of SAE 15W-40 (John Deere TY6391).

Elements	Weight (%)	IP (kJ/mol)	Psat	
			torr	°C
Ca	0.29	590	$\sim 10^{-8}$	282
Zn	0.14	960	8×10^{-4}	280
P	0.13	419	1	261
Mg	0.04	738	$\sim 10^{-5}$	282
S	0.33	1000	1	189
C		1087	$\sim 10^{-8}$	1657
Fe		762	$\sim 10^{-8}$	892

show that the metals in the form of isolated metal-rich spherules primarily consist of Ca rather than other metal elements. Actually, this is not that big of a surprise because S, the most abundant species, are likely to exist in vapor phase due to their high saturation vapor pressure (Table 1).

Figure 6 shows that the morphology of the DPM with dose of lube oil is pretty similar to that of the Fe-doped DPM. EDS measurements for DPM denoted by circle in the figure clearly show that the dark areas in DPM contain a lot of Ca and the nuclei mode particles are self-nucleated hydrocarbon and metal rich particles.

This figure also shows, perhaps better than Figure 5, that the light gray particles, i.e. organic carbon particles are more abundant than metal-rich nuclei.

4.2. Species Size Distribution

More than 500 mass spectra for each condition were collected and analyzed by our own computer program that is able to search and analyze peaks in a mass spectrum, and thereby estimate contents of the elements

composing a parent particle. Such given total area of peaks versus time of flight in a mass spectrum is converted to volume equivalent size of the corresponding particle by an adequate volume-peak area correlation (Lee *et al.*, 2005). The whole analyses for 500 mass spectra data is finished within half an hour. We can extract any statistical relations from a collection of the analysis results. This is a unique and striking benefit of single particle analysis and makes the SPMS so useful in nanotechnology and any research fields dealing with nanoparticles as well.

4.2.1. Fe-doped DPM

Before looking at detailed particle stoichiometry, we present the SPMS results for the three classes of DPM (explained in the previous section), in terms of the frequency distribution of each class as a function of particle size. Figure 7(a) shows that at low engine load and high ferrocene doping rate, the "elemental carbon" particles are widely distributed, with a peak at around 70 nm, and constitute the bulk of the particulate material, which coincides with the distribution of agglomerate particles i.e. the accumulation mode particles shown in Figure 3(a). Figure 7(a) also shows that the "organic carbon" particles are distributed in the lower size range (< 50 nm) i.e. the lower-side tail of the accumulation mode. Under the conditions for Figure 7(a) we see virtually no "pure iron" particles. This is probably due to higher carbon generation at low load, preferentially facilitating Fe adsorption onto carbon particles rather than nucleation of Fe. The result is that at the lower load, the nuclei-mode iron particles as measured by mobility diameter (Figure 3a), are fewer in number and almost all less than 30 nm in diameter, and in that range the mass-spectrometer has poor particle transmission efficiency (Mahadevan *et al.*, 2002).

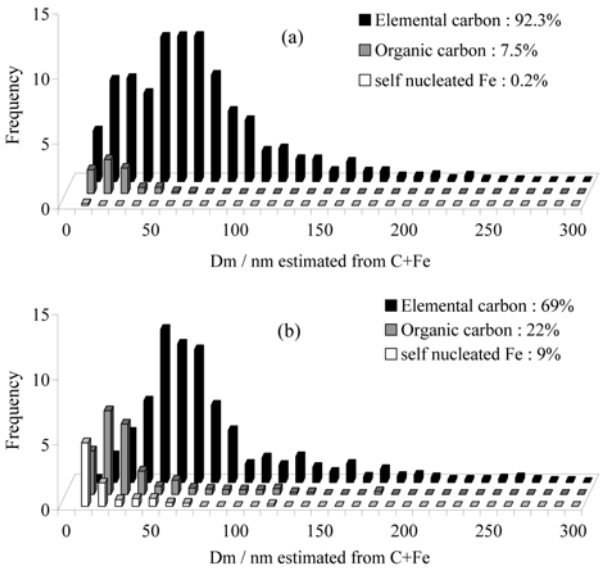

Figure 7. Size distributions of three species of DPM doped with 60 ppm Fe at (a) 0 kW; (b) 6 kW engine load.

At higher engine load, the increase in Fe throughput combined with inherent soot reduction yields a higher Fe/C ratio, so the pure iron particles have increased in number and grown in size to a point where the aerodynamic lens is able to transmit them more efficiently to the ionization laser. Figure 7(b) shows that at 6 kW engine load, about 9% of the detected particles (by number) are pure iron nanoparticles. Note that in this figure the size distribution of the elemental carbon particles has not changed significantly, which is consistent with the SMPS measurement in Figure 3(a).

4.2.2. 1% Lube oil-doped DPM

When various metals in the form of lube oil are added to the fuel, the species distribution is somewhat different from the previous. Three interesting things are found in this case as follows: 1) no distinct self-nucleation of metals even at higher total dose of metals, 2) dominance of Ca rich particles even in accumulation mode, i.e. they are not just in the nuclei mode, 3) apparent under-estimation of nuclei mode particles as compared to in the iron doping case. All points are essentially inter-related through the thermo-physical properties (vapor pressure) of metal and the mechanism of metal formation. Though more Ca is added than Fe, the higher vapor pressure of Ca enables it to exist in vapor phase for a longer time period during the expansion process. The vapor thus has time to condense into the preexisting DPM rather than self nucleate as in the case for Fe. This is a possible route for Ca forming.

But, here one may raise an issue related to the amount of Ca exceeding the other species (contained in the oil) and even carbon. Elemental carbon seems very likely to be much more reduced due to the high dose and the catalytic effect of Ca (compare Figures 3 and 4). The function of Ca for enhancing carbon oxidation was demonstrated with thermo-gravimetric analysis by Miyamoto *et al.* (1998). Also, since much of the sulfur leaves the tail-pipe as vapor-phase SO_2 due to its high vapor pressure, only a few percent of sulfur is known to convert to particulate sulfate. Thus, the recondensed Ca may be primary species detected by SPMS.

Unfortunately, we are not in a position to give an answer as to whether Ca is self-nucleated or not, because it is also possible that the Ca particles in the accumulation mode may have resulted from violent coagulation between self-nucleated Ca particles. There remains another question, why the big nuclei-mode peak in Figure 4 is not shown in Figure 8, which is not consistent with Fe-doped DPM. We would note that the size measured by SMPS is

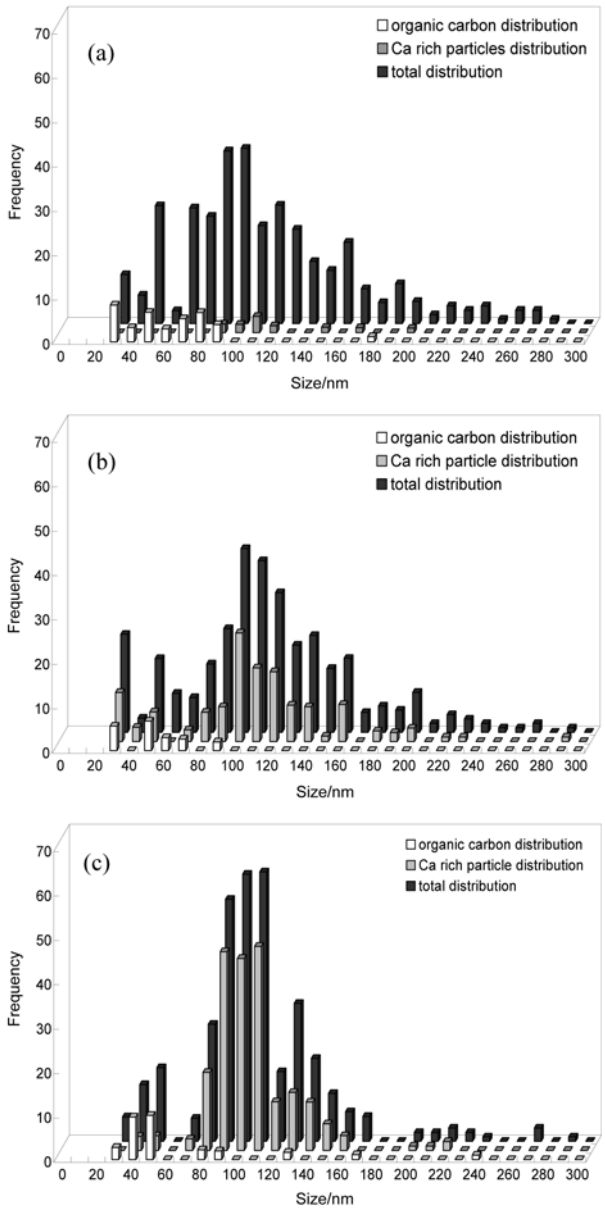

Figure 8. Size distributions of three species of DPM doped with 1 % lube oil at (a) 0 kW; (b) 2 kW; (c) 6 kW engine loads.

electrical mobility size (~aerodynamic size), while the size measured by SPMS is volume equivalent size. In other words, even if the Fe rich and Ca rich particles have the same aerodynamic size and pass though the aerodynamic lens with similar transmission efficiency, the heavier Fe rich particles can have smaller volume. Therefore, in contrast to the Ca, the detectable volume-equivalent size range of Fe particles with the SPMS spans to smaller size. This may be the answer to the question posed in the third point (apparent underestimation of

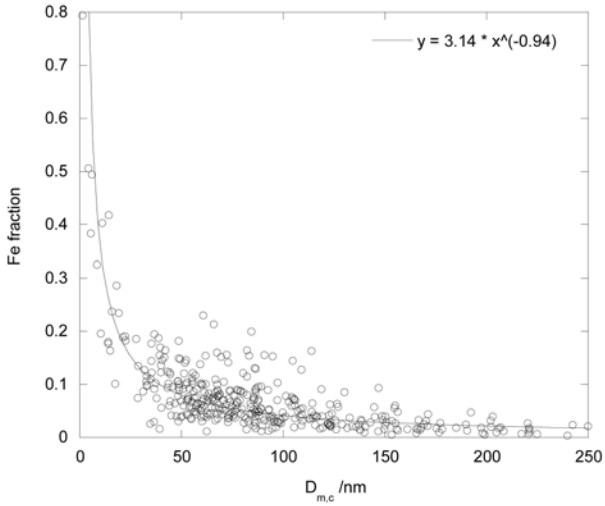

Figure 9. Metal fraction in 20 ppm Fe-doped DPM as a function of carbon core size at 0 kW engine load.

nuclei mode).

4.3. Stoichiometry of Species in Metal-doped DPM

To confirm the above-mentioned mechanism of metal formation, we draw a plot of metal-to-carbon ratios against carbon core size for a large number of particles. Figure 9 demonstrates that the ratio is strongly correlated with the preexisting carbon core size and proportional to $D_{m,c}^{-0.94}$. Note that the diameter $D_{m,c}$ representing mobility size of the carbon core is estimated only from the carbon contents in the mass spectra with a mass spectra-to-size converting formula (Lee *et al.*, 2005). Also, note that in the free molecular regime, the recondensation rate of volatile species is proportional to the surface area of preexisting particles, while in the continuum regime it is proportional to the size. In turn, the ratio should have size dependence of $D_{m,c}^{-2}$ for the free molecular regime or $D_{m,c}^{-1}$ for the continuum regime. The proximity of the dependence to $D_{m,c}^{-1}$ reflects that the iron vapors condense onto the carbon cores during the rapid expansion process inside engine, where the pressure is still high. On the other hand, as engine load or the amount of dose increases, nucleation and subsequent coagulation between nuclei and carbon agglomerates make the data scattered from the correlation seen in Figure 9. This becomes more pronounced at all condition of lube-oil doping case, which is explained mainly by the higher dose of metals.

5. CONCLUSIONS

We demonstrate for the first time that single particle mass spectroscopy can be successfully used to characterize individual diesel exhaust particles in terms of size and composition. From the datasets, we extract several

interesting relations which are meaningful in statistical view. When small amounts of metal are introduced to the engine as fuel additives, the metal vapor from the disintegration of metals in the engine condenses onto the pre-existing carbon spherules somewhere during the expansion process inside the engine. As more metals are added, the governing mechanism is shifted from condensation to nucleation and subsequent coagulation between nuclei and pre-formed agglomerates. The relative dominance between nucleation and coagulation is determined by not only the dose of metals but thermo-physical properties of metal vapor.

ACKNOWLEDGEMENT–This work is part of the project "Development of Partial Zero Emission Technology for Future Vehicle" and is also supported by the Core Environmental Technology Development Project for Next Generation (Project No. 102-041-029). We are grateful for these financial supports.

REFERENCES

Gross, D. S., Galli, M. E., Silve, P. J., Wood, S. H., Liu, D.-Y. and Prather, K. A. (2000). Single particle characterization of automobile and diesel truck emissions in the Caldecott tunnel. *Aerosol Sci. Technol.,* **32**, 152–163.

Higgins, K. J., Jung, H., Kittelson, D. B., Roberts, J. T. and Zachariah, M. R. (2003). Kinetics of diesel nanoparticle oxidation. *Environ. Sci. Technol.*, **37**, 1949–1954.

Jung, H., Kittelson, D. B. and Zachariah M. R. (2005). The influence of a cerium additive on ultrafine diesel particle emissions and kinetics of oxidation. *Comb. Flame.,* **142**, 276–288.

Jung, H., Kittelson, D. B. and Zachariah, M. R. (2003). The influence of engine lubricating oil on diesel nanoparticle emissions and kinetics of oxidation. *SAE Paper No.* 2003-01-3179.

Kim, S. H., Fletcher, R. A. and Zachariah, M. R. (2005a). Understanding the difference in oxidative properties between flame and diesel soot nanoparticles: the role of metals. *Environ. Sci. Technol.,* **39**, 4021–4027.

Kim, H., Lee, S., Kim, J., Cho, G., Sung, N. and Jeong, Y. (2005b). Measurement of size distribution of diesel particles: effects of instruments, dilution methods, and measuring positions. *Int. J. Automotive Technology* **6**, **2**, 119–124.

Kittelson, D. (1998). Engines and nanoparticles: a review. *J. Aerosol Sci.,* **29**, 575–588.

Kittelson, D., Johnson, D. and Watts, W. (2002). Diesel Aerosol Sampling Methodology, *CRC E-43 Final Report* available at http://www.crcao.com, Georgia, USA.

Kyto, M., Aakko, P., Nylund, N.-O. and Niemi, A. (2002). Effect of lubricant on particulate emissions of heavy duty diesel engines. *SAE Paper No.* 2002-01-2770.

Lee, D., Park, K. and Zachariah, M. R. (2005). Determination of size distribution of polydisperse nanoparticles with single particle mass spectrometry: the role of ion kinetic energy. *Aerosol Sci. Technol.,* **39**, 162–169.

Mahadevan, R., Lee, D., Sakurai, H. and Zachariah, M. R. (2002). Measurement of condensed-phase reaction kinetics in the aerosol phase using single particle mass spectrometry. *J. Phys. Chem. A,* **106,** 11083–11092.

Miyamoto, N., Zhixin, H. and Hideyuki, O. (1998). Catalytic effects of metallic fuel additives on oxidation characteristics of trapped diesel soot. *SAE Paper No.* 881224.

Noble, C. A. and Prather, K. A. (2000). Real-time single particle mass spectrometry: a historical review of a quarter century of chemical analysis of aerosols. *Mass Spectrum. Rev.,* **19,** 248–274.

Park, K., Lee, D., Rai, A., Mckherjee, D. and Zachariah, M. R. (2005). Size-resolved kinetic measurements of aluminum nanoparticle oxidation with single particle mass spectrometry. *J. Phys. Chem. B,* **109**, 7290–7299.

Sakurai, H., Tobias, H. J., Park, K., Zarling, D., Docherty, K. S., Kittelson, D. B., McMurry, P. H. and Ziemann, P. J. (2003). On-line measurements of diesel nanoparticle composition and volatility. *Atmospheric Environment,* **37**, 1199–1210.